J|A|C|S
ARTICLES
Published on Web 07/19/2006

Formation of Nearly Monodisperse In_2O_3 Nanodots and Oriented-Attached Nanoflowers: Hydrolysis and Alcoholysis vs Pyrolysis

Arun Narayanaswamy,[†] Huifang Xu,[‡] Narayan Pradhan,[†] Myeongseob Kim,[†] and Xiaogang Peng*,[†]

Contribution from the Department of Chemistry and Biochemistry, University of Arkansas, Fayetteville, Arkansas 72701, and Department of Geology and Geophysics, and Materials Science Program, University of Wisconsin, Madison, Wisconsin 53706

Received April 20, 2006; E-mail: xpeng@uark.edu

Abstract: Single crystalline and nearly monodisperse In_2O_3 nanocrystals with both dot and flower shapes were synthesized in a simple reaction system. This system used indium carboxylates as the precursors with or without alcohol as the activating reagents in a hydrocarbon solvent under elevated temperatures. Limited ligand protection (LLP) led to three-dimensional (3D) oriented attachment of nanodots, resulting in 3D nanoflowers. When the system had sufficient ligand protection for the nanocrystals, nanodots were found to be the stable products. The diameters of nearly monodisperse nanodots and nanoflowers were varied in a range from ~5 to ~15 nm and ~15 to ~60 nm, respectively. The simple reaction system made it possible to have a systematic study of the reaction mechanisms along with the growth kinetics of nanocrystals. Hydrolysis and alcoholysis were identified as the major paths for this system, as opposed to pyrolysis. Both nearly monodispersed nanodots and nanoflowers can be made through either of the reaction pathways. Hydrolysis was found as a reversible pathway, and alcoholysis was confirmed to be irreversible. Consequently, a sufficient amount of alcohol was able to force the yield of nanocrystals, both dots and flowers, to unity.

Introduction

Synthesis of nanocrystals with a defined size[1−3] and shape[4−10] has advanced dramatically in recent years, to which high temperature approaches (roughly 250−350 °C) in organic solvents, either through organometallic schemes[1,5,11] or alternative approaches (or greener approaches),[12−14] have played a key role and often been regarded as the mainstream synthetic chemistry in the field. Emphasis on synthetic chemistry of nanocrystals is currently moving into nano-objects with complex structures and compositions,[15] and formation of three-dimensional (3D) colloidal nanocrystals is especially underdeveloped. This report intends to illustrate a detailed mechanistic study for the formation of complex 3D structures for In_2O_3 nanocrystals, monodisperse nanodots vs nanoflowers, through a greener approach. The results will illustrate that although similar approaches are frequently referred to as pyrolysis or thermolysis of precursors under elevated temperatures, the actual reaction pathways are hydrolysis and alcoholysis for this particular system. Using either of these two pathways, the reaction system can be tuned to generate monodisperse nanodots or nanoflowers with different sizes by simply varying the degree of ligand protection for the nanocrystals. Specifically, formation of nanoflowers through 3D oriented attachment was observed in an interesting growth domain, a limited ligand protection (LLP) domain, while the reaction in the traditional sufficient ligand protection domain yielded high quality nanodots.

Development of the mainstream synthetic chemistry for 0D and one-dimensional (1D) structures has been greatly benefited by the mechanistic studies on growth of the corresponding nanostructures. The case for 1D nanostructure synthesis will be discussed in the next paragraph as an example. However, all these studies are mostly limited to growth

[†] University of Arkansas.
[‡] University of Wisconsin.

(1) Murray, C. B.; Norris, D. J.; Bawendi, M. G. *J. Am. Chem. Soc.* **1993**, *115* (19), 8706−15.
(2) Peng, X.; Wickham, J.; Alivisatos, A. P. *J. Am. Chem. Soc.* **1998**, *120* (21), 5343−5344.
(3) O'Brien, S.; Brus, L.; Murray, C. B. *J. Am. Chem. Soc.* **2001**, *123* (48), 12085−12086.
(4) Trentler, T. J.; Hickman, K. M.; Goel, S. C.; Viano, A. M.; Gibbons, P. C.; Buhro, W. E. *Science* **1995**, *270* (5243), 1791−4.
(5) Peng, X.; Manna, U.; Yang, W.; Wickham, J.; Scher, E.; Kadavanich, A.; Alivisatos, A. P. *Nature* **2000**, *404* (6773), 59−61.
(6) Pacholski, C.; Kornowski, A.; Weller, H. *Angew. Chem., Int. Ed.* **2002**, *41* (7), 1188−1191.
(7) Tang, Z.; Kotov, N. A.; Giersig, M. *Science* **2002**, *297* (5579), 237−240.
(8) Peng, Z. A.; Peng, X. *J. Am. Chem. Soc.* **2002**, *124* (13), 3343−3353.
(9) Lee, S.-M.; Cho, S.-N.; Cheon, J. *Adv. Mater.* **2003**, *15* (5), 441−444.
(10) Cho, K.-S.; Talapin, D. V.; Gaschler, W.; Murray, C. B. *J. Am. Chem. Soc.* **2005**, *127* (19), 7140−7147.
(11) Cho, K.; Koh, H.; Park, J.; Oh, S. J.; Kim, H.-D.; Han, M.; Park, J. H.; Chen, C. T.; Kim, Y. D.; Kim, J. S.; Jonker, B. T. *Phys. Rev. B: Condens. Matter Mater. Phys.* **2001**, *63* (15), 155203/1−155203/7.
(12) Peng, Z. A.; Peng, X. *J. Am. Chem. Soc.* **2001**, *123* (1), 183−184.
(13) Sun, S.; Zeng, H. *J. Am. Chem. Soc.* **2002**, *124* (28), 8204−8205.
(14) Jana, N. R.; Chen, Y.; Peng, X. *Chem. Mater.* **2004**, *16* (20), 3931−3935.
(15) Peng, X.; Thessing, J. *Struct. Bonding* **2005,** *118* (Semiconductor Nanocrystals and Silicate Nanoparticles), 79−119.

10.1021/ja0627601 CCC: $33.50

kinetics,[15] and systematic information on the chemical reaction mechanisms for a typical synthetic process has been rarely reported. This is probably why the organometallic and the greener approaches are commonly called "pyrolysis" or "thermolysis" of the precursors under high temperatures. When one is interested in developing general strategies for synthesis of 3D complex nanostructures, such systematic mechanisms about the involved chemical reactions might become critical, provided the expected complex structure changes in the reaction system. Synthetic schemes involved in the formation of oxide nanocrystals should be a good starting point for such studies as the synthetic system can be extremely simple, as simple as the thermal treatment of a fatty acid salt in a hydrocarbon solvent,[14] to be discussed here. In addition, such chemical reaction information shall also provide valuable references for understanding reactions involved in formation of other types of inorganic nanocrystals in the mainstream synthetic chemistry. At present, metal fatty acid salts are rapidly becoming the most common precursors used in synthesis of all types of inorganic nanocrystals in nonaqueous media under elevated temperatures. Presumably, thermal stability of these precursors under synthetic conditions is of great importance for designing and understanding any of these synthetic schemes.

The importance of the crystal growth mechanism discussed above might be illustrated with the example of synthetic chemistry for 1D nanowires, i.e., solution−liquid−solid approaches[4] and 1D oriented attachment.[6,7,10,16−18] For 1D oriented attachment, the electric dipole moment of the nanocrystals has been found to play a determining role. The dipole moment of a given type of crystal has a given set of possible orientations as indicated by a recent impressive study in Murray's group,[10] which thus generates nanorods/wires and related structures with a given set of orientations.

Nanocrystals with complex 3D structures are interesting for solar cells, catalysis, sensing, and other surface/shape related properties and applications.[19,20] For instance, CdTe and other semiconductor tetrapods[21,22] are ideal structures for fabrication of high performance solar cells.[23] Such tetrapods, however, were typically formed by a traditional path, atom by atom growth from nuclei, and the intrinsic crystal structures seem to play a key role. Thus, it is not clear how to extend the synthetic methods to different structures. Some reports indicate that nanodots and nanorods can self-assemble into different complex shaped particles.[24−26] Such complex structures, however, were often quite large, fragile, and/or polycrystalline. Some other reports indicated possibilities for formation of complex nanostructures through 3D attachment, although these reports were typically brief, missing clear mechanistic evidences, or structurally not well characterized.[27] Thus, a general pathway to reach 3D oriented attachment has not yet been achieved.

In_2O_3 and related materials, such as indium tin oxide (ITO), are probably the most frequently used transparent conductors[28−32] and commercialized hosts for various sensing devices.[20,33−36] In_2O_3 nanocrystals may improve the performance in these major types of applications. Implementation of In_2O_3 nanocrystals may reduce the fabrication costs of transparent conductors. These nanomaterials, especially 3D nanoflowers, can also offer a substantially large surface area for sensing. Some successful approaches have been reported for the synthesis of high quality In_2O_3 nanodots.[37−39] As pointed out above, the approach presented here is significantly simpler, which involves indium carboxylate salt decomposition in a generic hydrocarbon solvent (octadecene, ODE) with or without activation by a long chain alcohol. A similar approach has been proven to be successful for transition metal oxide (Fe_3O_4, MnO, etc.)[14] and post-transition metal oxide (ZnO) nanocrystals.[40] Experimental data for In_2O_3 nanocrystals to be discussed below, a model system for main group oxides, revealed some interesting new insights for this general approach. In this regard, identification of hydrolysis as a pathway in this nonaqueous system under temperatures as high as 290 °C was a surprise to us. The main difference between the two identified pathways, hydrolysis vs alcoholysis, is that hydrolysis is a reversible process while esterification through alcoholysis is not. It was possible to control the system to go through just one of the pathways, with the esterification pathway giving a close to unity yield of nanocrystals.

Results

Choice of the synthetic system was more or less straightforward. Past experiences taught us that octadecene (ODE) should be a reasonable solvent because it is a liquid at room temperature but with a high boiling point, inert to oxide formation, not very toxic, and inexpensive (actually less expensive than toluene). Using a noncoordinating solvent, as to be demonstrated below, allowed us to realize 3D attachment by simply tuning the concentration of the ligands in the reaction

(16) Penn, R. L.; Banfield, J. F. *Science* **1998**, *281* (5379), 969−971.
(17) Yang, H. G.; Zeng, H. C. *Angew. Chem., Int. Ed.* **2004**, *43* (44), 5930−5933.
(18) Yu, J. H.; Joo, J.; Park, H. M.; Baik, S.-I.; Kim, Y. W.; Kim, S. C.; Hyeon, T. *J. Am. Chem. Soc.* **2005**, *127* (15), 5662−5670.
(19) Gur, I.; Fromer, N. A.; Geier, M. L.; Alivisatos, A. P. *Science* **2005**, *310* (5747), 462−465.
(20) Pinna, N.; Neri, G.; Antonietti, M.; Niederberger, M. *Angew. Chem., Int. Ed.* **2004**, *43* (33), 4345−4349.
(21) Manna, L.; Milliron, D. J.; Meisel, A.; Scher, E. C.; Alivisatos, A. P. *Nat. Mater.* **2003**, *2* (6), 382−385.
(22) Yu, W. W.; Wang, Y. A.; Peng, X. *Chem. Mater.* **2003**, *15* (22), 4300−4308.
(23) Huynh, W. U.; Dittmer, J. J.; Alivisatos, A. P. *Science* **2002**, *295* (5564), 2425−2427.
(24) Chen, J.; Herricks, T.; Xia, Y. *Angew. Chem., Int. Ed.* **2005**, *44* (17), 2589−2592.
(25) Liu, B.; Zeng, H. C. *J. Am. Chem. Soc.* **2004**, *126* (26), 8124−8125.
(26) Tzitzios, V.; Niarchos, D.; Gjoka, M.; Boukos, N.; Petridis, D. *J. Am. Chem. Soc.* **2005**, *127* (40), 13756−13757.
(27) Zitoun, D.; Pinna, N.; Frolet, N.; Belin, C. *J. Am. Chem. Soc.* **2005**, *127* (43), 15034−15035.
(28) Puetz, J.; Al-Dahoudi, N.; Aegerter, M. A. *Adv. Eng. Mater.* **2004**, *6* (9), 733−737.
(29) Qadri, S. B.; Kim, H. *J. Appl. Phys.* **2002**, *92* (1), 227−229.
(30) Naghavi, N.; Marcel, C.; Dupont, L.; Rougier, A.; Leriche, J.-B.; Guery, C. *J. Mater. Chem.* **2000**, *10* (10), 2315−2319.
(31) Ederth, J.; Johnsson, P.; Niklasson, G. A.; Hoel, A.; Hultaker, A.; Heszler, P.; Granqvist, C. G.; van Doorn, A. R.; Jongerius, M. J.; Burgard, D. *Phys. Rev. B: Condens. Matter Mater. Phys.* **2003**, *68* (15), 155410/1−155410/10.
(32) Emons, T. T.; Li, J.; Nazar, L. F. *J. Am. Chem. Soc.* **2002**, *124* (29), 8516−8517.
(33) Williams, D. E. *Sens. Actuators, B: Chemical* **1999**, *57*, 1−16.
(34) Neri, G.; Bonavita, A.; Micali, G.; Rizzo, G.; Galvagno, S.; Niederberger, M.; Pinna, N. *Chem. Commun.* **2005**, (48), 6032−6034.
(35) Zhang, D.; Liu, Z.; Li, C.; Tang, T.; Liu, X.; Han, S.; Lei, B.; Zhou, C. *Nano Lett.* **2004**, *4* (10), 1919−1924.
(36) Kim, S.-R.; Hong, H.-K.; Kwon, C. H.; Yun, D. H.; Lee, K.; Sung, Y. K. *Sens. Actuators, B: Chemical* **2000**, *B66* (1−3), 59−62.
(37) Murali, A.; Barve, A.; Leppert, V. J.; Risbud, S. H.; Kennedy, I. M.; Lee, H. W. H. *Nano Lett.* **2001**, *1* (6), 287−289.
(38) Liu, Q.; Lu, W.; Ma, A.; Tang, J.; Lin, J.; Fang, J. *J. Am. Chem. Soc.* **2005**, *127* (15), 5276−5277.
(39) Seo, W. S.; Jo, H. H.; Lee, K.; Park, J. T. *Adv. Mater.* **2003**, *15* (10), 795−797.
(40) Chen, Y.; Kim, M.; Lian, G.; Johnson, M. B.; Peng, X. *J. Am. Chem. Soc.* **2005**, *127* (38), 13331−13337.

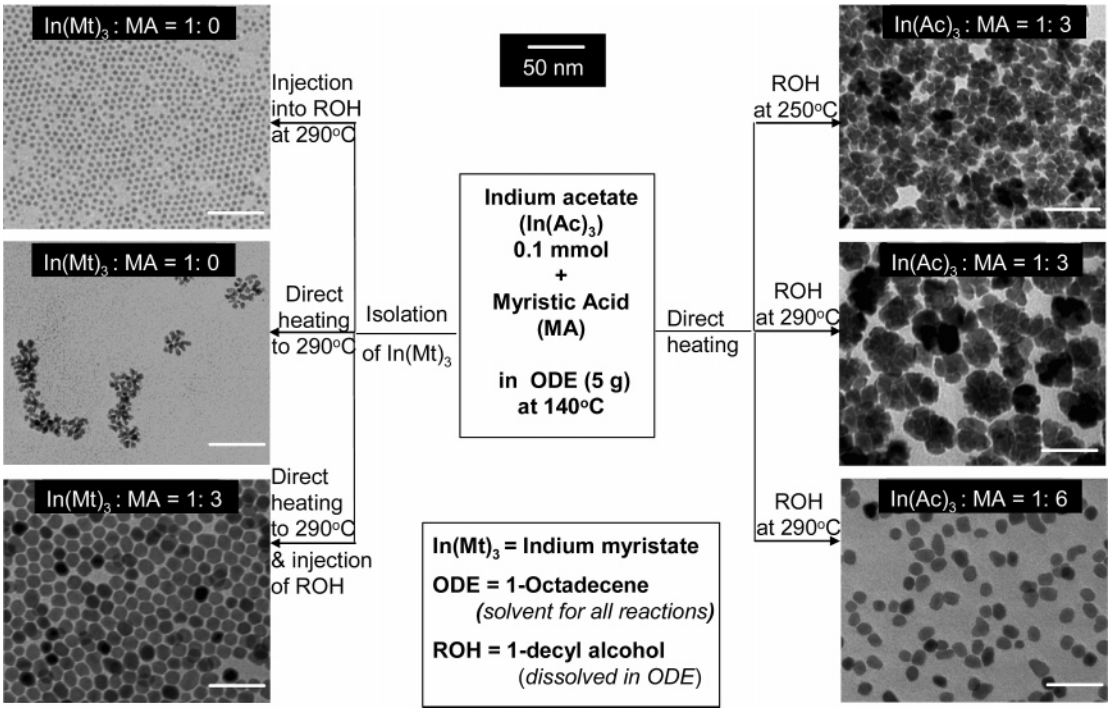

Figure 1. Reaction schemes and the representative TEM images of the resulting nanocrystals. *Note:* Because of boiling point concerns, the alcohol used in the injection reaction (top left) was octadecyl alcohol, instead of decyl alcohol used in other cases.

solution. The resulting products and reaction patterns of this simple system, however, seem to be significantly different from those observed in similar approaches for the synthesis of transition metal oxide and post-transition metal oxide nanocrystals.[14,40]

Indium acetate ($In(Ac)_3$) is probably the most readily available indium compound for a nonaqueous phase system and hence was logically selected as our starting material. However, our initial results indicated that direct reaction of $In(Ac)_3$ under elevated temperatures was complex. Other types of indium carboxylate salts, such as indium stearate ($In(St)_3$) and indium myristate ($In(Mt)_3$) were thus synthesized and used as precursors for understanding this interesting system. Results for fatty acid salts with different chain lengths were fairly the same, and the results pertaining to $In(Mt)_3$ will be given in detail along with the results for using $In(Ac)_3$.

Formation of In_2O_3 nanocrystals under different reaction conditions was studied systematically by varying the concentration of the ligands, the concentration of the precursors, the chain length of the ligands, the manner of introduction of precursors into the reaction system, the reaction temperature, time and temperature for the addition of alcohol, etc. Using myristic acid (MA) as the ligands, six typical reactions and the TEM pictures of the representative nanocrystals are summarized in Figure 1.

The synthetic reactions in Figure 1 can be classified into two groups. The reactions shown on the right side in Figure 1 were all related to the direct heating of the dissolved $In(Ac)_3$, in the presence of myristic acid as the ligands, to the desired reaction temperatures. Under the given conditions, $In(Ac)_3$ became soluble in ODE, only if fatty acids were added into the solution. To the left side, indium myristate ($In(Mt)_3$) was isolated, purified, characterized (see Supporting Information), and used as the precursor.

At first glance, the two groups of reactions, with or without the isolation of $In(Mt)_3$, seemed to be quite different from each other. However, there exists a general and interesting trend for both groups. When the concentration of ligands was low, the resulting nanocrystals were nanoflowers, single crystalline nanostructures with complex 3D morphology (a detailed structure will be given later). This can be easily seen by comparing the bottom two approaches on either side in Figure 1. When the concentration of MA was doubled, the resulting nanocrystals in both cases switched from nanoflowers to dots. To understand this better, reactions under different conditions were closely monitored by FTIR (Figure 2).

The temporal evolution of the FTIR spectrum for each typical reaction in Figure 1 is shown in Figure 2, with the left column and right column in Figure 2 corresponding to the left side and right side schemes in Figure 1, respectively. The assignments of the main IR vibration bands in the spectral window shown in Figure 2 are summarized in Table 1.

Although most assignments in Table 1 were straightforward, the carbonyl peak of carboxylic acid group (COOH) at about 1711 cm^{-1} was quite different from pure myristic acid which is typically found at about 1702 cm^{-1}. This variation can be explained by different hydrogen bonding environments for the carboxylic groups in the nonpolar reaction mixture and pure (solid) state.[42] To further confirm this, the side products of the related reactions (for example, the middle reaction on the left side, Figure 1) were isolated. The FTIR, ^{13}C NMR, and ^{1}H NMR spectra of the purified compound (Supporting Information) were found to be identical to those of pure myristic acid. Furthermore, the carbonyl vibration frequency of myristic acid in ODE upon heating also showed a similar shift. With these evidences, we concluded the assignment for this major peak, as shown in Table 1.

(41) Fresenius, W.; Huber, J. F. K.; Pungor, E.; Rechnitz, G. A.; Simon, W.; West, T. S. *Tables of Spectral Data for Structure Determination of Organic Compounds*, 2nd ed.; Springer-Verlag: Berlin, 1989.
(42) Bellamy, L. J. *The Infrared Spectra of Complex Molecules*, 3rd ed.; Chapman and Hall: New York, 1975.

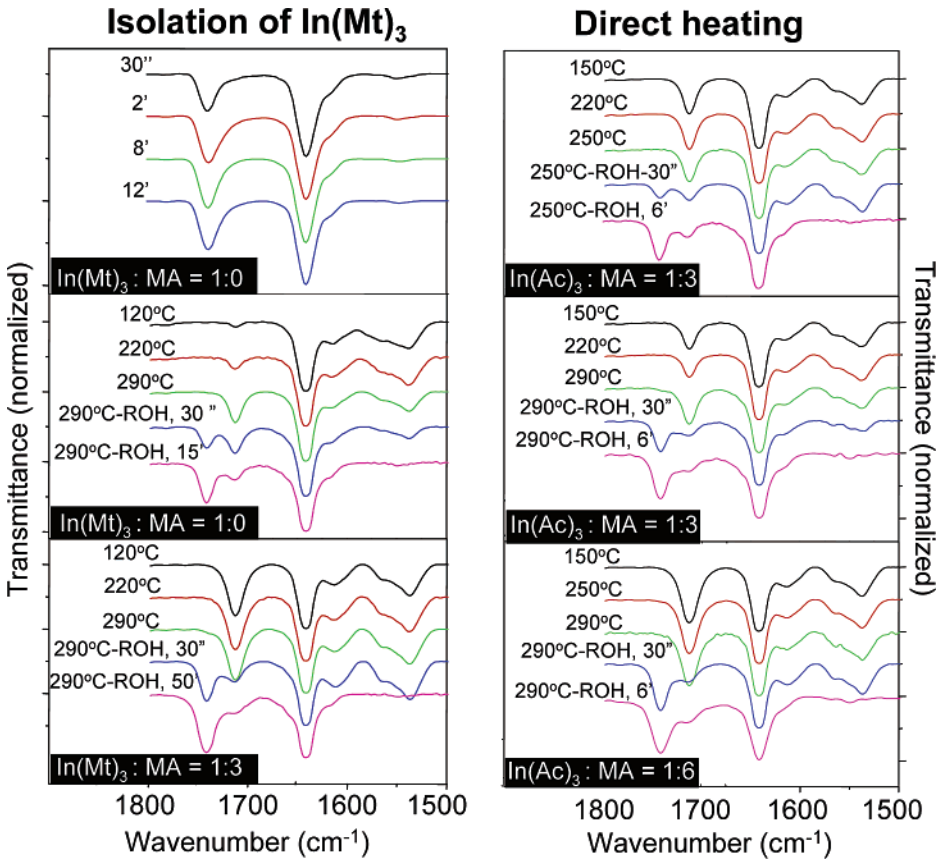

Figure 2. Temporal evolution of the FTIR spectrum for the six typical reactions shown in Figure 1. The plots in the left (right) column are for the reactions on the left (right) side in Figure 1 and follow the same order from top to bottom.

Table 1. IR Assignments

frequency (cm^{-1})	nature of the vibration	assignment methods
1539 and the shoulders at 1565 and 1607	COO^- asymmetric stretch	from ref 41
1642	C═C stretch	assigned by comparing with the standard IR spectrum of ODE
1711	C═O stretch from COOH	assigned by comparing with the standard IR spectrum of myristic acid in ODE
1739	C═O stretch from ester	from ref 41

All the spectra shown in each plot for a specific reaction in Figure 1 were normalized using the relatively intense C═C vibration band at 1642 cm^{-1} originating from ODE (the solvent) as the standard, which should be a constant during the entire course of the reaction. To make the FTIR data quantitatively reliable, it was necessary to spot the hot aliquots directly onto an IR substrate. This is so because the solubilities of the starting materials, products, and side products are substantially different from each other at room temperature, although they all were found to be soluble in ODE under elevated temperatures. Thus, dilution of the aliquots by any tested solvents resulted in quantitatively unreliable FTIR data. For instance, when $CHCl_3$ was used as the dilution solvent, the COO^- asymmetric vibration band was often falsely presented as the saturation concentration of the carboxylate salts in the solvent.

The replacement of acetate in $In(Ac)_3$ by myristate or other long chain carboxylates used in a specific reaction was expected to be completed above the boiling temperature of acetic acid. The FTIR data, however, indicate a quite different pattern. Upon heating to 140 °C, insoluble $In(Ac)_3$ disappeared and the entire reaction system became a clear solution. FTIR data indicate that even if the In:MA ratio was set as 1:3, just a sufficient amount of MA to replace all acetate, there was still a significant amount of COOH detected in the IR spectra (the first spectrum in the top and middle reactions on the right side in Figure 2) after the precursor became soluble. The intensity of this peak further decreased slightly upon heating to 250 °C and increased thereafter on further heating (to be discussed later). Since the boiling point of acetic acid is 120 °C, this vibrational band should come from the unconverted MA. If assuming each indium ion was coordinated with three carboxylate groups, the ratio of ligands between acetate and myristate was found to be around 1:2 as judged by the FTIR peak intensities. This indicates that the ligand replacement did not go to completion and the resulting soluble indium compound was a carboxylate salt with mixed ligands, roughly two myristate and one acetate per indium.

Reaction of the soluble indium carboxylate compounds was found to be strongly dependent on reaction conditions. When fatty acids, such as myristic acid, were in large excess (the bottom reaction on both sides, Figure 1), no observable changes were found by neither FTIR (the bottom plot on both columns in Figure 2) nor TEM (no particles being found) up to

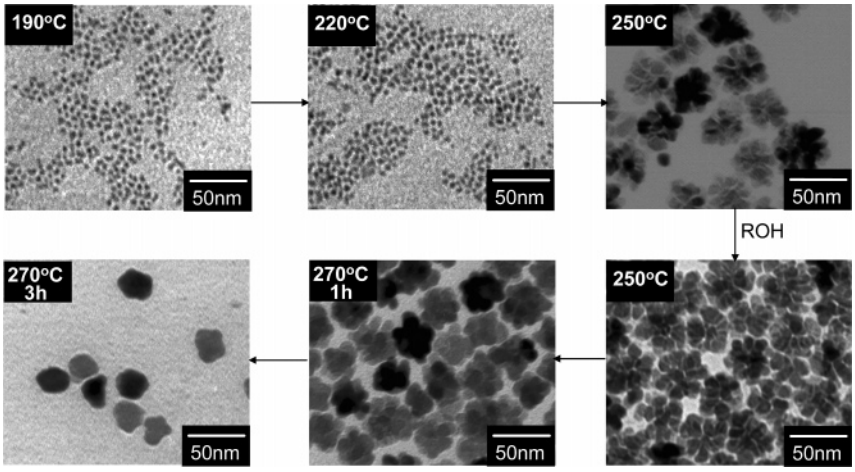

Figure 3. Temporal evolution of the morphology of the nanocrystals for a typical reaction carried at 250 °C (the top scheme on the right side in Figure 1).

290 °C in comparison to the case after the solution became clear. Literature indicates that indium acetate, similar to other acetates,[43] should decompose at 270 °C.[44] This observation thus has two implications. One, pyrolysis of the precursors was not occurring under the given conditions. Two, the soluble indium carboxylate compound for the direct heating case was chemically quite different from pure $In(Ac)_3$. This further indicates that one should be cautious to judge the reaction pathway when metal acetate salts are used as precursors, if other potential ligands exist.

When the $In(Ac)_3$:MA ratio was 1:3 (top and middle plots in Figure 2, right column), which is the theoretical amount of MA needed for replacement of all acetate, the carbonyl vibration of free acids increased when the temperature was higher than ~250 °C. This increase was accompanied by a decrease in the peak intensity for the asymmetric vibration bands of the carboxylate group. These changes were relatively small due to the complex chemical processes, replacing acetate by MA, evaporation of acetic acid, and hydrolysis of $In(Mt)_3$ (see details below). However, they became much more visible when purified $In(Mt)_3$ without the addition of any free MA was used (the middle plot in the left column in Figure 2). The rate of this conversion increased as the reaction temperature increased. At a given temperature, the system would reach a steady state with a fixed intensity ratio for the two vibrational bands, the one belonging to COOH and the other one corresponding to COO^-. The isolated compound giving the COOH vibrational band at 1711 cm^{-1} was confirmed to be free MA (Supporting Information).

The most plausible reaction which converts $In(Mt)_3$ to free MA should be the hydrolysis of the salt. For hydrolysis to be significant for the given reaction system, only ~1 mg of water would be needed theoretically. The purified $In(Mt)_3$ salts were found to possess visible IR features associated with water (Supporting Information). We failed to obtain anhydrous $In(Mt)_3$ without hydrolyzing the compound, despite vacuum-drying the purified product overnight. This implies that $In(Mt)_3$ might contain some structured water. Nevertheless, one reaction was carried out, for which the reaction system was pumped/purged with argon 3 times at 100 °C using standard protocol prior to heating to 290 °C. The formation of free acid was indeed found to be significantly slowed.

The IR spectra of the reaction mixture would eventually reach a steady state within the temperature range, with or without excess ligands, if no alcohol was added. In other words, under any conditions, the system could maintain a constant intensity for both COOH and carboxylate vibrations. This again indicates that the soluble indium carboxylate salts did not undergo spontaneous pyrolysis by themselves. As to be discussed later, the yielded free acid can actually react with In_2O_3 nanocrystals, the reverse reaction of hydrolysis. Therefore, the observed steady state should be the equilibrium state between hydrolysis of the indium salt and dissolution of the nanocrystals by the free acids.

The presence of alcohol changed the reaction path quite significantly. Formation of esters was evidenced by the rapid appearance of the strong carbonyl group for ester at about 1739 cm^{-1} and the complete disappearance of the COOH and COO^- vibrational bands within a few minutes at 290 °C (the last IR spectrum in each series in Figure 2 with the exception of the one in the top plot in the right column). At lower reaction temperatures, such as at 250 °C, this process occurred at a slower pace (the top plot in the right column in Figure 2).

It is interesting to compare the reactivity of zinc and indium carboxylate salts. Zinc salts do not undergo hydrolysis under the same conditions, and the dissolution of ZnO nanocrystals by free fatty acids was extremely fast.[40] This difference probably is the reason formation of high quality ZnSe and ZnS nanocrystals[45] did not require any substantial degassing in comparison to the synthesis of InP and InAs nanocrystals.[46] For both cases, injection of anionic precursors was carried out after the metal fatty acid salts were heated to at least 250 °C. At such temperatures, if a tiny amount of water existed, indium salts would partially undergo hydrolysis but zinc salts would be stable.

Three-dimensional (3D) oriented attachment was evidenced by the temporal evolution of the morphology of the nanocrystals (Figure 3) and also by their structural analysis which will be discussed below. Appearance of a small amount of dot-shaped nanocrystals was observed when hydrolysis just started in the temperature range 180−200 °C, and the particles grew slightly in size as the reaction temperature was increased (the first two images in Figure 3). At about 250 °C, nanoflowers

(43) Yin, M.; O'Brien, S. *J. Am. Chem. Soc.* **2003**, *125* (34), 10180−10181.
(44) *Aldrich Catalogue 2005−2006*; Sigma-Aldrich Co.: St. Louis, MO, 2005; p 1401.
(45) Li, L. S.; Pradhan, N.; Wang, Y.; Peng, X. *Nano Lett.* **2004**, *4* (11), 2261−2264.
(46) Battaglia, D.; Peng, X. *Nano Lett.* **2002**, *2* (9), 1027−1030.

became the dominating species with the disappearance of the dots. At the same time, the reaction mixture became slightly turbid but no precipitation occurred. If no heating or addition of alcohol was applied to the reaction system, the reaction remained stable without any visual change by either naked eye or TEM measurements. Addition of alcohol made the reaction mixture significantly more turbid, and still no precipitation was evidenced. TEM measurements indicated that the concentration of the nanoflowers was much higher than that before alcohol injection. Careful purification indicated that the turbidity was due to the light scattering caused by the nanoflowers, which were dispersible in nonpolar solvents as a stable colloidal solution. When the reaction temperature was increased to 270 °C, the nanoflowers became less pointed and more round. Continued heating at this temperature finally turned the nanoflowers to faceted and single crystalline dots (see high-resolution TEM (HRTEM) picture in the Supporting Information).

Not all stages of morphology evolution shown in Figure 3 could be observed in a complete sequence. For instance, the final conversion from nanoflowers to faceted dots might not be observed if the reaction temperature was set at 250 °C. If free fatty acids were not stable, being consumed within a few minutes at 290 °C and in the presence of alcohol, the nanoflowers could be very stable upon heating for at least 7 h. The latter fact indicates that the smoothing process and the transition of nanoflowers to nanodots involved the redissolution of the nanoflowers by the free fatty acids. In the case of ZnO nanocrystals, nanopyramids were dissolved to nanodots and zinc fatty acid salts by the addition of free fatty acids.[40] The resulting ZnO nanodots, however, would grow back to the nanopyramids by the reaction between the alcohol and the salts. Evidently, the resulting In_2O_3 nanodots were the stable species in this system and did not revert back to nanoflowers under any conditions tested. This is actually not a surprising result for oriented attachment. In a typical 1D oriented attachment, the surface of the pearl-shaped nanowires/nanorods often became smoother upon heating in an irreversible manner, thereby resulting in nearly perfect nanowires/rods.[47] For 3D structures, a similar smoothing process should result in faceted dots.

The results and discussions presented in the above paragraphs suggest that the smoothing process of the nanostructures formed by oriented attachment requires their surface atoms to be "mobile or removable" in the reaction solution. It would be interesting to confirm this hypothesis for a system undergoing 1D oriented attachment. Nevertheless, this hypothesis is consistent with our previous study for reversibility of ZnO nanocrystal growth.[40] It was observed that any intraparticle and Ostwald ripening requires the components of a crystallization system to be significantly soluble as monomers in the solution. Otherwise, the system will be permanently trapped in an arbitrary state, the nanoflowers for the current case.

Interestingly, even after exhausting the free ligands in the solution, the largely sized primary dots were unable to convert to nanoflowers. Prolonged heating in a large excess of alcohol might precipitate the dots, but no formation of nanoflowers was observed. Related to this, formation of nanoflowers always occurred in the early stages of a reaction with fresh and not so well developed dots. Furthermore, injection of indium precursors into hot alcohol−ODE solutions (Figure 1, top left) can yield

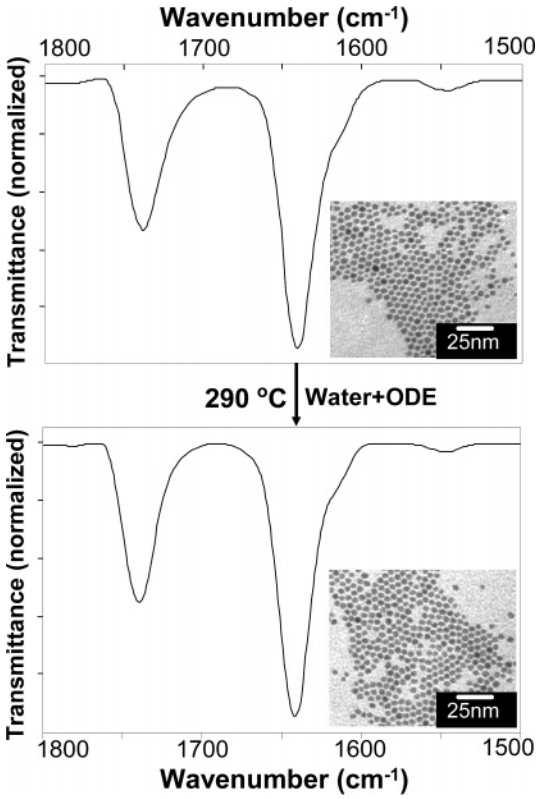

Figure 4. FTIR spectrum and TEM (inset) image before and after water addition.

nearly monodisperse dots, but these dots could not be converted to nanoflowers even if no excess ligands were present in the solution.

One may argue that this phenomenon, 3D oriented attachment always occurring in the early stage of a reaction, might be associated with the presence of a trace amount of water in the early stage of a reaction. After the reaction proceeded for a certain period of time, water would be mostly evaporated under such high temperatures, and thus the surface ligands became more stable because of lack of hydrolysis. Consequently, if the system did not enter into LLP in the early stage of the reaction, LLP and 3D oriented attachment would unlikely occur.

To test the above hypothesis, we made a batch of stable nanodots at 290 °C (Figure 4, top). After that, the nanocrystals were reacted with water by injecting a water−ODE mixture (5 mg of water in 1 g of ODE). The reaction went violent for ~2 min because of the boiling of water (Caution: water−ODE mixture should be added dropwise), indicating a sufficient amount of reaction time for the nanodots with water. However, the nanocrystals did not seem to change at all as observed by either FTIR or TEM measurements (Figure 4, bottom). This implies the above hypothesis was not correct.

The single crystalline nature of the nanoflowers and nanodots was confirmed by HRTEM observations (Figure 5). One typical HRTEM image of a nanoflower is shown in Figure 5 (left, top panel). The visible lattice fringes of all nanoflowers were found to run across the entire flower structure (insets in Figure 5, left), indicating oriented attachment of several particles to form the nanoflowers. Gaps between primary particles were visible (insets), but they did not interfere with the lattice orientation. As expected for random 3D attachment, there was no specific attachment axis identifiable by HRTEM. The nearly

(47) Pradhan, N.; Xu, H.; Peng, X. *Nano Lett.* **2006**, *6* (4), 720−724.

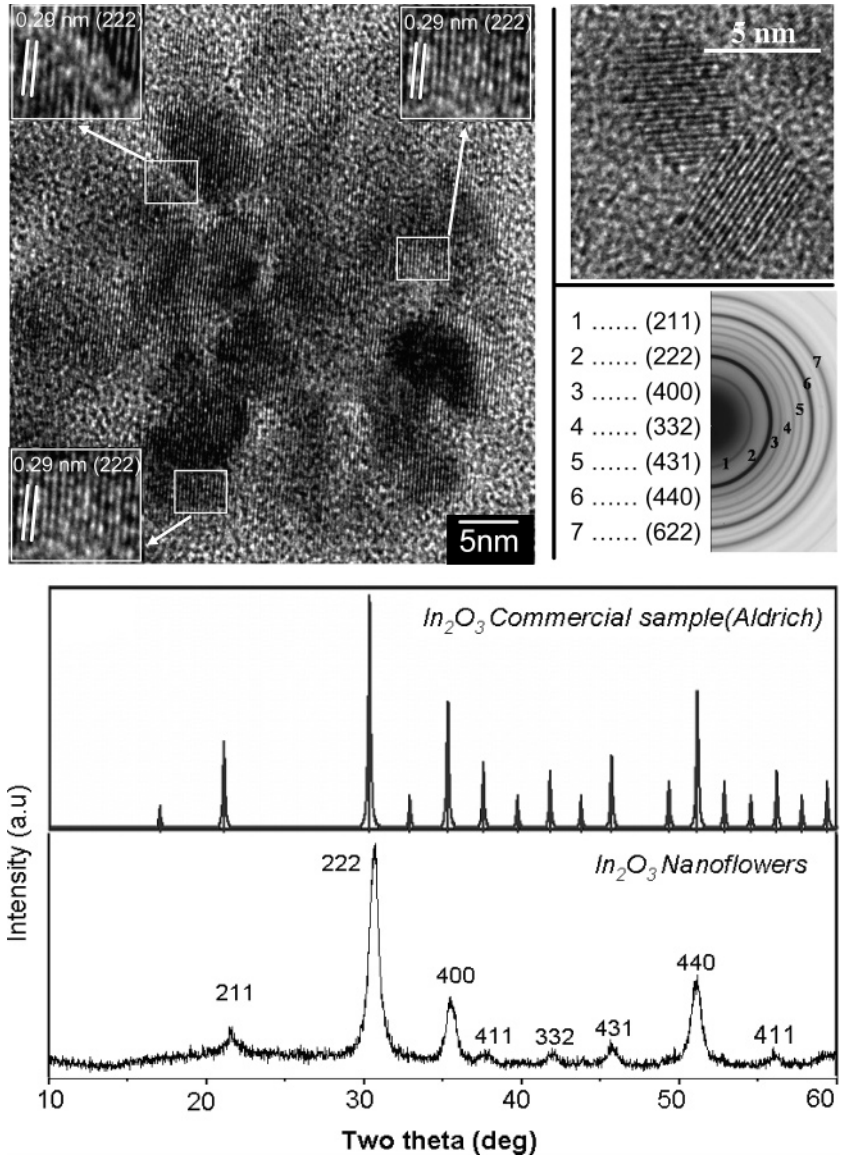

Figure 5. Top panel: HRTEM images of a representative nanoflower (left) and two nanodots (top right). Both flowers and dots showed the same electron diffraction (bottom right). Bottom panel: X-ray powder diffraction patterns of bulk In_2O_3 (top) and nanoflowers (bottom).

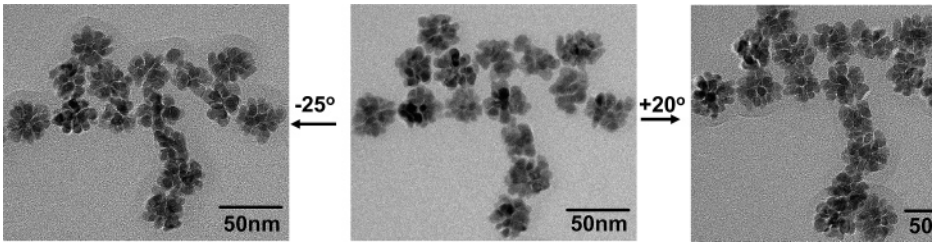

Figure 6. Rotation of a group of nanoflowers.

monodisperse nanodots were also single crystalline in nature. Both nanoflowers and nanodots were found to have the same diffraction pattern identified by electron diffraction (Figure 5, bottom right, top panel) and X-ray diffraction (Figure 5, bottom panel), which corresponded to the cubic phase of In_2O_3.

The 3D nature of the nanoflowers was further confirmed by rotation experiments shown in Figure 6. When the specimen was rotated either way (left and right image), the two-dimensional projection of each nanoflower roughly remained the same, but the structural detail of each flower changed substantially. This indicates that the nanoflowers are true three-dimensional structures, instead of plates with their thickness different from their diameter. The rotation experiments and HRTEM observations further imply that each nanoflower was formed by geometrically random but lattice-oriented attachment of multiple primary nanocrystals.

The size of both nanodots and nanoflowers, without multiple injections of precursors and size sorting, can be varied

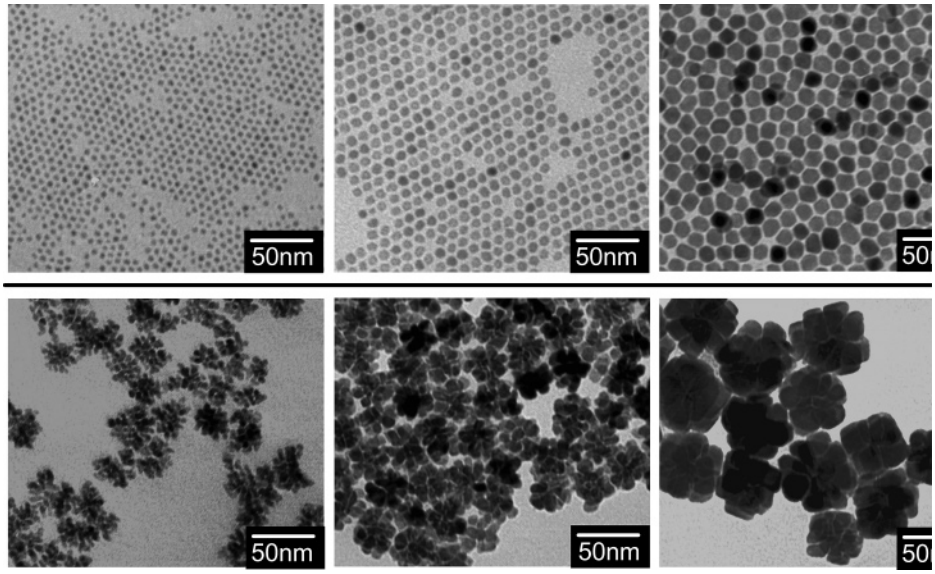

Figure 7. TEM images of nanodots and nanoflowers with different sizes.

by changing the initial reaction conditions (Figure 7). Nearly monodisperse nanodots were synthesized in the size range between ~4 and ~15 nm. Nanoflowers with a decent size distribution were formed in the size range between ~15 and ~60 nm. The yield of either nanodots or nanoflowers was close to unity, if an esterification reaction was applied. The reactions generating nanodots as the sole products were the ones with excess fatty acid ligands no matter which reaction route, hydrolysis or esterification, the system went through. Typically, smaller nanodots were formed at shorter reaction times. A higher concentration of alcohol yielded smaller nanodots probably because the rapid esterification reaction generated more nuclei. A lower monomer concentration also gave smaller nanocrystals. Finally, injection of purified indium fatty acid salt precursors into alcohol at higher reaction temperatures, i.e., 290 °C, yielded smaller dot-shaped nanocrystals. Injection of alcohol to a mixture of indium fatty acid salt precursor and the corresponding fatty acid results in the formation of bigger nanocrystals. Smaller nanoflowers were observed when a relatively low monomer concentration was used. Fatty acid ligands with a long hydrocarbon chain often yielded nanoflowers with larger diameters. Nanoflowers formed in the early stages were more pointed, which became more round after prolonged heating (Figure 3).

3D oriented attachment of nanocrystals with various compositions was examined.[48] The experimental results of the In_2O_3 model system discussed above indicate that, under low ligand concentrations and/or with short ligands, 3D oriented attachment occurred. This trend sounds plausible. When nanocrystals were not sufficiently protected by organic ligands, aggregation seemed to be a reasonable pathway for minimizing the surface energy of nanocrystals.[49] We suggest this growth mechanism to be named as "limited ligand protection" (LLP). The detailed results for LLP for different types of nanocrystals will be reported separately.

It should be pointed out that Kotov's group observed a similar phenomenon for 1D oriented attachment.[7] In their case, CdTe nanocrystals showed oriented attachment only after a purification process that supposedly removed some ligands in the system. The results demonstrated above imply that it should be possible to control the occurrence of oriented attachment without additional purification steps if a system has a mechanism to control the degree of protection provided by the ligands to the nanocrystals.

Discussions

Neither indium acetate nor other fatty acid salts of indium underwent pyrolysis as normally suggested. Instead, hydrolysis and esterification (with addition of alcohol) were identified as possible pathways. We did not use amines as activation reagents mainly because of two reasons. It is environmentally appealing to have a synthetic system only containing C, H, and O in addition to the necessary targeted components of the nanocrystals, In and O in this case. In addition, amines were often found to be both activation reagents and ligands. Alcohol used in this system, however, did not bind to the surface of the nanocrystals as ligands (see Supporting Information), which makes it easier to understand the mechanism.

The main reactions observed in this given system can be summarized as follows:

$$\mathrm{In(Ac)_3 + RCOOH \xrightarrow{\Delta} In(RCOO)_{\mathit{x}}(Ac)_{3-\mathit{x}} + HAc\uparrow} \quad (1)$$

$$\mathrm{\underset{\text{or } In(RCOO)_3}{In(RCOO)_{\mathit{x}}(Ac)_{3-\mathit{x}}} + H_2O \overset{\Delta}{\rightleftharpoons} In_2O_3 + RCOOH} \quad (2)$$

$$\mathrm{\underset{\text{or } In(RCOO)_3}{In(RCOO)_{\mathit{x}}(Ac)_{3-\mathit{x}}} + R'OH \xrightarrow{\Delta} In_2O_3 + RCOOR'} \quad (3)$$

In_2O_3 represents the resulting nanocrystals irrespective of their shapes. The reversibility of eq 2 was responsible for the formation of round flowers and their subsequent conversion into faceted dots. For the formation of nanoflowers, excess ligands should be avoided. This is so because excess ligands will provide

(48) Narayanaswamy, A.; Xu, H.; Pradhan, N.; Kim, M.; Peng, X. *Angew. Chem., Int. Ed.* **2006**, in press.
(49) Mullin, J. W. *Crystallization*, 3rd ed.; Butterworth-Heinemann: Oxford, 1993; p 480.

sufficient ligand protection for the yielded nanocrystals (see Figure 1), which pushes the system to be out of the LLP mode.

Generally speaking, nanoflowers are a thermodynamically unstable species. If there were sufficient ligands in the system to make the monomers mobile, either on the surface or in the solution, nanoflowers would transform into dot-shaped nanocrystals (Figure 3). When the monomers were reasonably stable in solution (mobile on the surface), the nanocrystals go through Ostwald (intraparticle) ripening. However, since eq 3 is irreversible, free acids could be consumed rapidly and completely if sufficient alcohol was present in the system. This was responsible for the stability of the nanoflowers in the high-temperature synthesis (290 °C). On the contrary, complete conversion of the nanoflowers to faceted nanodots (Figure 3) was observed at relatively lower temperatures. Consistent with this, the existence of free fatty acids for a long period of time, even after the addition of alcohol, was evidenced in the top plot in the right column in Figure 2.

Since eq 3 is fast and also irreversible, the addition of alcohol could convert all free fatty acids and fatty acid salts into the corresponding esters. The free fatty acids underwent the reverse reaction in eq 2 first and then followed eq 3 to become esters. The irreversibility of eq 3 also made the yield of the nanocrystals to be unity. This was similar to the case for the ZnO nanocrystal system studied in our group.[40]

Recent results on 1D oriented attachment strongly suggest that the dipole moments of primary nanocrystals play a key role for the formation of 1D nanowires.[6,7,10] This hypothesis has been convincingly supported by the systematic and quantitative analysis for the case of PbSe nanowires.[10] The results in this work indicate that the dipole moment may not be the only driving force for oriented attachment. In principle, if oriented attachment occurred in 3D randomly, the driving force must be more or less homogeneous in three dimensions. Following the general expression of Gibbs's Law, the driving force for crystal growth is to minimize the total surface free energy of a system.[49] Certainly, oriented attachment would do so, and the oriented feature should further limit the interface energy between primary particles.

Kotov's group, however, revealed that removal of excess ligands in the system plays a key role in the formation of CdTe nanowires through 1D oriented attachment.[7] The results in this work further imply that a synthetic system may be directly controlled in the oriented attachment regime by using a limited amount of ligands. This is actually reasonable. If the primary nanocrystals are well surrounded by organic ligands, it would be difficult for the lattice of a nanocrystal to interact with others. Even if the ligands on the surface of nanocrystals are dynamically bound, primary nanocrystals would be more sterically isolated in a solution with more free ligands.

In our study an interesting phenomenon was observed, whereby nearly monodispersed nanocrystals formed either by injection or direct heating did not undergo oriented attachment even after there were no free ligands left in the system. A related fact mentioned in the Results section was that formation of nanoflowers was always observed in the early stages of a reaction with not so well-developed primary dots. These facts may indicate that nanocrystals with relatively high surface energy may be more "suited" for oriented attachment.

Based on the above discussion, one may depict the 3D oriented attachment in a synthetic system as follows. When a system starts with an insufficient amount of ligands, below the critical ligand concentration for stabilization of individual nanocrystals at a given temperature, the freshly formed primary nanocrystals may undergo 3D aggregation. The insufficient surface ligand coverage provides the needed kinetic driving force for 3D oriented attachment. Although dipole moment plays an additional role, probably sometimes also being a substantial role, in the kinetics of 1D oriented attachment, it should not be as important as insufficient surface ligand coverage in the case of 3D oriented attachment. During the growth of nanocrystals, formation of 3D aggregates should always be thermodynamically favorable because of the reduced surface free energy of the individual crystals. The excessively high surface energy of each not so well-developed primary nanocrystal forms the energetic driving force for the subsequent 3D oriented attachment. If the enthalpy gain from such oriented attachment dominates the entropy loss, 3D oriented attachment becomes thermodynamically favorable.

The key issue for designing a system which is capable of generating both monodisperse nanodots and 3D complex structures is to identify the critical ligand protection point. This point is determined by the concentration and bulkiness of the ligands. Above the critical ligand protection point, monodisperse and stable nanodots can be yielded as the sole product. Below such a critical point, the freshly formed nanodots with high free surface energy rapidly become unstable after they are formed because of LLP. Subsequently, they aggregate to form 3D objects. The high surface free energy might further drive the primary nanocrystals to undergo oriented attachment to form the 3D aggregates, if the enthalpic gain dominates the entropic loss as discussed above.

Conclusion

In summary, a synthetic system can be manipulated to yield monodisperse nanocrystals with either a dot or flower shape. For the In_2O_3 model system, 3D oriented attachment yields single crystalline flower-shaped nanocrystals. If the system provided sufficient ligand protection for the resulting nanocrystals, the products will be dot-shaped. On the contrary, LLP (limited ligand protection) resulted in nanoflowers. For the In_2O_3 model system studied here, LLP occurred in both identified pathways, hydrolysis and alcoholysis. Systematic studies on reaction mechanisms, coupled with studies on traditional growth kinetics of nanocrystals, reveal that pyrolysis was not observed with the reaction temperature as high as 290 °C. Our preliminary results on other oxide systems, such as MnO and ZnO, also support this conclusion. These results indicate that our overall view for the current mainstream synthetic methods for high quality nanocrystals[15] might need to be reconsidered.

Experimental Section

Materials. Indium acetate ($In(Ac)_3$), myristic acid (MA), stearic acid, decyl alcohol, and 1-octadecene (ODE, tech 90%) were purchased from Aldrich. 1-Octadecyl alcohol (ODA) was purchased from Alfa Aesar. All chemicals were used without further purification.

Synthesis of Indium Myristate ($In(Mt)_3$). In a typical reaction $In(Ac)_3$ (10 mmol) was treated with MA (40 mmol) and heated to 140 °C under an argon atmosphere. The mixture was heated for 6 h, and then the product was isolated by addition of acetone. The resulting

precipitate was filtered, dried, and again treated with MA (40 mmol) to ensure complete conversion of acetate to myristate. The final product ($In(Mt)_3$) was washed several times with acetone to remove excess MA, dried, and used as a precursor. The product was characterized by FTIR and ^1H NMR (see Supporting Information).

Synthesis of Indium Stearate ($In(St)_3$). The synthetic method was similar to the one for $In(Mt)_3$, except MA was replaced by SA.

Synthesis of In_2O_3 Nanoflowers and Shape Transition. In a typical reaction $In(Ac)_3$ (0.1 mmol), MA (0.3 mmol), and 5 g of ODE were loaded in a 25 mL three-necked flask. The mixture was degassed and heated to 250 °C under an argon atmosphere. Within 5 min of reaching 250 °C, the reaction mixture became slightly turbid. Decyl alcohol (0.3 mmol) dissolved in 0.25 g of ODE was quickly injected into the above mixture at this temperature. Within 2−5 min of addition of decyl alcohol, the reaction mixture became more turbid without any signs of precipitation. The reaction was monitored by FTIR and TEM by taking aliquots at different temperatures enroute to 250 °C and also at different time intervals at 250 °C. The nanoflowers formed were ∼30 nm in diameter. After the formation of nanoflowers as indicated by TEM, the temperature was raised to 270 °C and the nanoflowers were incubated for 3 h to form faceted nanodots.

Smaller nanoflowers (15 nm diameter) were formed by injection of decyl alcohol (0.06 mmol in 0.25 g ODE) into a mixture containing $In(Ac)_3$ (0.02 mmol), MA (0.06 mmol), and 4.75 g of ODE at 250 °C.

Similarly bigger nanoflowers (∼60 nm in diameter) were synthesized by using stearic acid (SA) in place of myristic acid. Typically, $In(Ac)_3$ (0.1 mmol), SA (0.3 mmol), and ODE (4.75 g) were heated to 290 °C, and then decyl alcohol (0.3 mmol in 0.25 g of ODE) was injected.

Synthesis of Stable Dot-Shaped In_2O_3 Nanocrystals. (a) Injection of Precursors. Stable dot-shaped (4−8 nm) In_2O_3 nanocrystals were formed by direct injection of pure $In(Mt)_3$ or $In(St)_3$. Typically ODA (3 mmol) and ODE (4.5 g) were loaded in a 25 mL three-necked flask, degassed, and heated to 290 °C. A solution of $In(Mt)_3$ or $In(St)_3$ (0.1 mmol) in 0.5 g of ODE is prepared separately by degassing and heating to 120 °C and then swiftly injected into the above solution at 290 °C. The resulting mixture was incubated for 30 min. Aliquots were taken at different time intervals after injection of the precursor for montitoring size by TEM.

(b) Injection of Alcohol into Pure $In(Mt)_3$. Bigger dot-shaped nanocrystals (∼15 nm in diameter) were synthesized by injecting decyl alcohol into a mixture of $In(Mt)_3$ and MA in ODE. In a typical experiment, decyl alcohol (0.5 mmol in 0.25 g of ODE) is injected into a mixture containing $In(Mt)_3$ (0.1 mmol) and MA (0.3 mmol) in 4.75 g of ODE. The reaction was incubated for 1 h to yield dot-shaped nanocrystals of ∼15 nm.

(c) Injection of Alcohol to $In(Mt)_3$ Formed in Situ by Reacting $In(Ac)_3$ and MA. Dot-shaped nanocrystals were also formed by the injection of decyl alcohol (0.5 mmol in 0.25 g of ODE) into a mixture containing $In(Ac)_3$ (0.1 mmol) and MA (0.6 mmol) in 4.75 g of ODE at 290 °C.

Fourier Transform Infrared Spectroscopy (FTIR). FTIR spectra were obtained on a Bruker Tensor 27 spectrophotometer. The specimens were prepared by directly spotting hot aliquots of a reaction mixture onto a NaCl crystal. This was done to obtain quantitatively reliable data for understanding the reaction. Dilution of the aliquots with solvents such as $CHCl_3$ and hexane was avoided because the solubilities of the starting materials, products, and side products were quite different from each other at room temperature.

Transmission Electron Microscopy (TEM). TEM and high-resolution TEM images were taken on a JEOL X-100 at 100 kV and Tecnai F30 field emission gun scanning transmission electron microscope equipped with an X-ray energy-dispersive spectroscopy (EDS) system. Point-to-point resolution of the HRTEM is 0.19 nm. Samples for JEOL X-100 were prepared by dipping a Formvar coated copper grid into a toluene solution containing the purified nanocrystals or into a hexane solution containing the aliquots taken during the course of a reaction. Selected area diffraction (SAED) was taken with a camera length of 120 cm. Specimen for HRTEM were prepared by depositing a drop of toluene solution containing the nanocrystals onto holey carbon-coated Cu grids.

X-ray powder diffraction patterns were obtained on a Philips PW1830 X-ray powder diffractometer using a Cu Kα line ($\lambda = 1.5418$ Å). The bulk In_2O_3 powder purchased from Aldrich was used as a reference.

Purification of In_2O_3 Nanocrystals (Nanodots and Nanoflowers). In_2O_3 nanocrystals were synthesized through the same procedure as that described above. The reaction mixture was cooled to 30 °C; 20 mL of ethyl acetate were used to precipitate indium oxide nanocrystals, and the nanocrystals were collected by centrifugation. The nanocrystals were then dispersed in toluene, and any insoluble residue was removed by centrifugation. In_2O_3 nanocrystals were precipitated by acetone and collected by centrifugation.

Acknowledgment. Financial support from the National Science Foundation (XP) and Alumni Research Foundation of the University of Wisconsin-Madison (HX) is acknowledged.

Supporting Information Available: TEM images of nanocrystals formed using stearic acid; ^1H NMR and FTIR spectrum of as-synthesized $In(Mt)_3$; ^1H NMR, ^{13}C NMR, and FTIR spectrum of isolated myristic acid; HRTEM of faceted dot from Figure 3 of the manuscript; and ^1H NMR of ligands on the surface of In_2O_3 nanocrystals. This material is available free of charge via the Internet at http://pubs.acs.org.

JA0627601